Valence determination as a function of doping in $PrBa_2Cu_3O_7$

U. Staub
Swiss Light Source, Paul Scherrer Institute, CH-5232 Villigen PSI, Switzerland

L. Soderholm and S. R. Wasserman
Chemistry Division, Argonne National Laboratory, Argonne, Illinois 60439

A. G. O. Conner and M. J. Kramer
Ames Laboratory, U.S. Department of Energy, Iowa State University, Ames, Iowa 50011

B. D. Patterson and M. Shi
Swiss Light Source, Paul Scherrer Institute, CH-5232 Villigen PSI, Switzerland

M. Knapp
Material Sciences, Darmstadt University of Technology, D-64287 Darmstadt, Germany
(Received 12 July 1999)

We present results of x-ray absorption near edge spectra (XANES), neutron powder diffraction, and resonant x-ray diffraction on samples of $PrBa_2Cu_3O_{7-\delta}$ and $Pr_{1-x}Ca_xBa_2Cu_3O_7$. The data are obtained as a function of the doping levels of oxygen and Ca. There are significant changes in the Pr L_3 XANES spectra with changes in oxygen or Ca concentrations, indicating that the Pr electronic properties are affected by doping. The resonant x-ray scattering experiments show that the changes observed occur on Pr ions incorporated in the $PrBa_2Cu_3O_{7-\delta}$ structure, and are not the result of changes to a Pr-containing impurity phase. A quantitative model, based on literature precedent, is used to extract Pr valences from the data, although the XANES cannot distinguish between models involving charge transfer and those involving hybridization. The results are compared with data obtained from $Pb_2Sr_2Pr_{1-x}Ca_xCu_3O_8$. The implications of these experiments are discussed in view of the exceptional magnetic and electronic properties of $PrBa_2Cu_3O_{7-\delta}$.

INTRODUCTION

Since the discovery of high-temperature superconductivity in series of rare-earth copper oxides, isostructural members that do not superconduct have attracted considerable interest. In particular $PrBa_2Cu_3O_7$, which is the isostructural analog of the $RBa_2Cu_3O_7$ series (R=Y or rare earth), is neither metallic nor superconducting.[1] This is in stark contrast to the other rare-earth analogs, which have superconducting transition temperatures $T_c \approx 90$ K. When Pr replaces Y to form the solid solutions $Y_{1-x}Pr_xBa_2Cu_3O_7$, T_c decreases with increasing Pr content, such that superconductivity is lost at $x \approx 0.55$. In addition to its anomalous conductivity behavior, $PrBa_2Cu_3O_7$ has an anomalously high antiferromagnetic ordering temperature[2] of the Pr moments, with a $T_N = 17$ K. This T_N is approximately an order of magnitude higher than for other rare earths in this series.[3,4] The high ordering temperature is accompanied by an anomalously short Pr to plane-oxygen distance in the chain (b) direction.[5] The high T_N suggest a strong superexchange mechanism. The shorter Pr-O distance may indicate a significant overlap between the Pr $4f$ wave functions and selected oxygen orbitals and/or an intermediate valent Pr. Inelastic neutron scattering experiments have been used to study the crystal-field splitting of the Pr ground multiplet and have determined a quasitriplet ground state which is slightly split but strongly broadened.[6–8] The strongly broadened lines are a further indication of strong hybridization and/or slight intermediate valence of the Pr ions.

Many proposals have been put forward to describe the suppression of superconductivity by Pr, including hole filling by charge transfer, a pair breaking mechanism involving the Pr magnetic moment, hybridization of the Pr states with the CuO_2 bands, and hole localization on the oxygen site due to changes of the electronic band structure driven by Pr-O orbital overlap.[9–13] The recent, unconfirmed observation of superconductivity in single crystals synthesized by the traveling-solvent floating-zone method[14,15] further complicates any understanding of the role played by Pr in the suppression of T_c.

Superconductivity observed in other isostructural members of the $YBa_2Cu_3O_{7-\delta}$ series is dependent on the oxygen content of the sample. When the oxygen content is low (i.e., $\delta \geqslant 0.5$), the samples are neither metallic nor do they superconduct. This behavior can be understood from a simple charge balance model. The additional charge induced by increasing the oxygen content is compensated by copper in one of its two sublattices, i.e., the chains or the planes. At low oxygen content, the average valence of copper is less than 2, such that all of the Cu in the CuO planes are Cu^{2+}, and there are no carriers for superconductivity. The Cu on the chains is reduced below divalency to maintain charge neutrality. At an oxygen content of $\delta = 0.5$, all the Cu is on average divalent. Increasing the oxygen content above 6.5 ($\delta \geqslant 0.5$) results in the oxidation of the planar Cu, thereby introducing holes as charge carriers. Although the oxygen content can be varied in $PrBa_2Cu_3O_{7-\delta}$, the samples do not become super-

conducting, even at high oxygen content. The issue at hand is whether or not Pr changes the electronic structure of the CuO planes, mimicking the effect of reducing oxygen content. A similar argument can be put forward for the substitution by Ca^{2+} of Pr. Mixed (Y/Ca/Pr)$Ba_2Cu_3O_7$ samples have been used to study the combined effects of Pr and Ca doping. Thin films of $Pr_{0.5}Ca_{0.5}Ba_2Cu_3O_7$ superconduct with a T_c of 47 K, which is higher than that[16] of $Pr_{0.5}Y_{0.5}Ba_2Cu_3O_7$. The data on Ca doping have been used to argue that T_c suppression by Pr cannot be solely explained by hole localization.

X-ray absorption near edge structure (XANES) is an excellent tool with which to probe the electronic states of rare-earth ions.[17] Several x-ray absorption studies on the Pr L_3 edge have been reported, investigating the valence state of Pr in $PrBa_2Cu_3O_7$. Whereas some of these experiments have been interpreted in terms of purely trivalent Pr,[18,19] others have reported indications[20–24] of intermediate valent Pr. Studies utilizing soft x-ray absorption experiments on the oxygen K edge have found a significant hybridization between the oxygen O $2p_\pi$ orbitals and the Pr $4f$ orbitals.[25] Unfortunately, commonly found impurity phases, such as $PrBaO_3$ or PrO_2, can influence such data, thus further complicating the analyses and interpretation.

In this work, we report on a detailed x-ray absorption investigation at the Pr L_3 edge of $Pr_{1.05-x}Ca_xBa_{1.95}Cu_3O_{7-\delta}$ for which we see a change in the XANES data as a function of doping. Resonant diffraction results on the same samples demonstrate that the changes in the XANES data result from Pr that is incorporated in the $PrBa_2Cu_3O_{7-\delta}$ structure. These results are interpreted using the existing models describing the anomalous properties of $PrBa_2Cu_3O_{7-\delta}$ and $(Pr_{1-x}Ca_x)Ba_2Cu_3O_7$.

EXPERIMENTS

$(Pr_{1.05-x}Ca_x)Ba_{1.95}Cu_3O_7$ samples were synthesized using dried Pr_6O_{11}, barium and calcium carbonate, and copper oxide. The copper oxide was heated in oxygen to 800 °C to full oxidation. The initial grinding was performed in a micromill, in order to reduce the particle size and to speed diffusion processes. The powder was calcined three times in CO_2-free air for 24 to 48 h, with intermediate grinding. Differential thermal analysis (DTA) and x-ray diffraction (XRD) were used after each heat treatment to check the phase purity. Calcinations were repeated until XRD and DTA data confirmed the formation of single-phase solid materials. The calcined samples were then annealed in either a 1 or 100 % oxygen atmosphere. The 100% pO_2 samples were annealed at 940 °C while the 1% samples were annealed at 900 °C due to differences in phase stability for different O_2 partial pressures. Oxygen soaks were done on ground powders at 450 °C for 48 h. XRD patterns reveal a systematic decrease in cell volume from 177.449 down to 176.145 Å^3 as the Ca content is increased to 0.15. Between $x=0.15$ and 0.2, there is an obvious second phase in the XRD. dc magnetization measurements show only paramagnetic behavior, with T_N becoming broader with increasing Ca content.

X-ray absorption spectra were obtained in both fluorescence and transmission modes at beamline $X10C$ at the National Synchrotron Light Source of Brookhaven National Laboratory. The beamline was equipped with a Si ⟨220⟩ double-crystal monochromator. Higher order harmonics were rejected with the use of a Pt coated mirror. Fluorescence spectra were collected with a 13 element Ge solid state detector cooled to liquid nitrogen temperature. The energy window of the individual detectors was set to collect only the high energy tail of the Pr (αL_{III}) emission line in order to reduce contamination from the Ba L_1 edge (βL_{I}) emission line located lower in energy by 150 eV. The resolution of the Ge detector was approximately 300 eV. The energy calibration was maintained by simultaneously monitoring a PrO_2 standard in the back channel. Except for differences in the Ba L_1-edge contamination at approximately 6003 eV, the transmission and fluorescence data are identical.

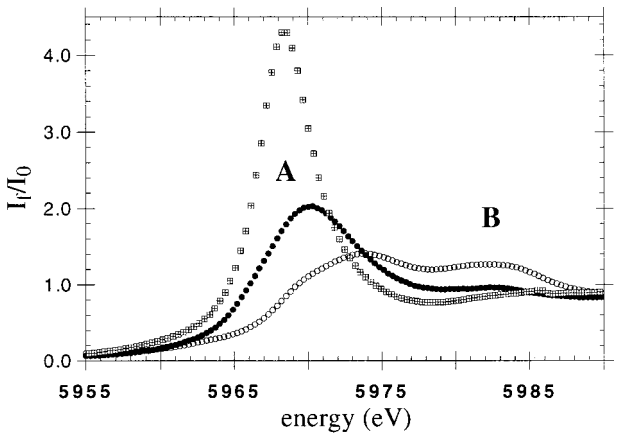

FIG. 1. X-ray absorption near edge structure (XANES) of the Pr L_3-edge in $Pr_{1.05}Ba_{1.95}Cu_3O_{6.97}$ (filled circles), in formally tetravalent Pr in PrO_2 (open circles), and in trivalent Pr in PrF_3 (crossed squares), taken in fluorescence mode at ambient temperature. The features A and B are discussed in the text.

The resonant powder diffraction data were collected at the Hasylab $B2$ beamline in Hamburg, using two rectangular (5×40 cm) image plates that together covered the 2θ range of 10°–135°. Energy calibration and intensity normalization were performed by adding Si powder to the sample and normalizing to the d spacings and intensities of the Si ⟨311⟩, ⟨331⟩, and ⟨400⟩ reflections. A finely ground sample glued externally to a 1 mm diameter quartz capillary reduced sample absorption for the x rays with energy approximately 6 keV. The full length of the x-ray path from the Be window to the image plate was evacuated in order to reduce absorption and air scattering.

RESULTS

A. Oxygen doping

Figure 1 compares the Pr L_3 edge XANES data of $Pr_{1.05}Ba_{1.95}Cu_3O_{6.97}$, PrF_3, and PrO_2. Purely trivalent Pr has a single resonance located at approximately 5970 eV, whereas formally tetravalent Pr, as found in PrO_2, exhibits a more complicated spectrum that can be described as two strong resonances, designated peak A and peak B, at approximately 5974 and 5982 eV, as well as some weaker features.[26,27] Whereas the underlying origin of the complex XANES spectra observed for tetravalent Ce and Pr compounds is not well understood, the general form of the two-peak feature at the edge energy is well established.[27,28] A

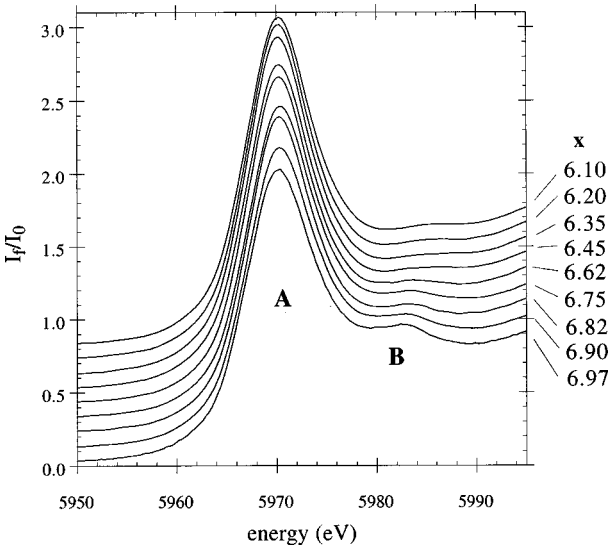

FIG. 2. Oxygen dependence of the Pr L_3-edge XANES in $Pr_{1.05}Ba_{1.95}Cu_3O_{7-\delta}$ taken in fluorescence mode. An offset of 0.1 has been added for decreasing oxygen content between each of the spectra. The features A and B are described in the text.

comparison of the PrF_3 and PrO_2 spectra, which are considered representative of trivalent and tetravalent Pr, respectively, with that obtained from the fully oxygenated $Pr_{1.05}Ba_{1.95}Cu_3O_{6.97}$ sample reveals a weak feature at approximately 5983 eV that is not present in the trivalent standard. This extra feature is a strong indication of either significant Pr-O hybridization or a slight Pr intermediate valence.

The oxygen dependence of the Pr L_3-edge XANES spectra is shown in Fig. 2. A comparison between these spectra reveals that peak B, which is associated with the presence of tetravalent Pr, increases with increasing oxygen content (decreasing δ). In addition, this peak is observed to shift to lower energy. The feature B is very weak for the undoped $Pr_{1.05}Ba_{1.95}Cu_3O_{6.1}$ sample. The samples with the three lowest oxygen contents have spectra that are indistinguishable, indicating that the electronic configuration of the Pr ions is unaffected by oxygen doping in the low doping regime. In order to quantify the changes to the XANES spectra observed at higher oxygen concentrations, we follow literature precedent on the interpretation of Pr XANES data.[27] The peak shown as B in Figs. 1 and 2 is defined as arising from a contribution from Pr^{4+}, or more precisely, peak A is a contribution from a $4f^2L$ configuration, and peak B is from a $4f^1$ configuration. In other words, Pr^{4+} $(4f^1)$ also has a contribution in its XANES spectrum from a charge transfer or hybridized state involving the Pr $4f$ states and the planar O $2p$ states. Using this model, in which Bianconi defines the valence of Pr as $v=3+I_B/(I_A+I_B)$, it is then possible to assign the changes seen in the Pr L_3 edge XANES to quantitative changes in valence. A quantitative analysis of the XANES data has been performed by fitting each spectrum with an arctan step function and two Lorentzians to represent the features A and B. For a better representation over a larger energy window, we introduced an additional Lorentzian and arctan function to describe the contributions from the Ba L_1 edge and the first EXAFS modulation at approximately 6003 eV. A linear background has been added to compensate for possible normalization errors. The total function has been convolved with a Gaussian resolution function. Fitting the L_3 edge data in this manner, we obtain the estimation of Pr valence shown in Fig. 8. Also included in Fig. 8 is the valence calculated by normalizing the XANES to the value obtained for PrO_2 of $v=3.44$. PrO_2 was chosen because Pr in this compound has a formal oxidation state of 4+. In this way we obtain an estimate of localized holes by Pr in $Pr_{1.05-x}Ca_xBa_{1.95}Cu_3O_7$.

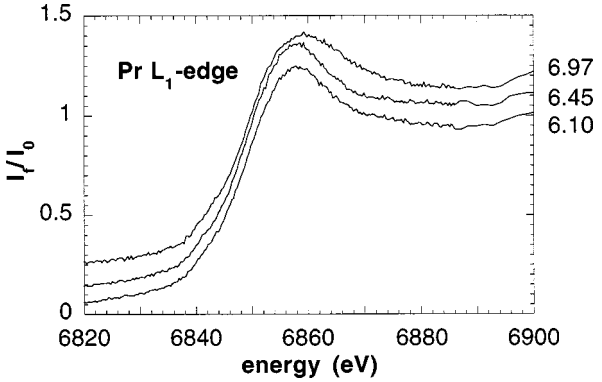

FIG. 3. Pr L_1-edge XANES of $Pr_{1.05}Ba_{1.95}Cu_3O_{7-\delta}$ for different oxygen contents δ, taken in fluorescence mode. An offset of 0.1 has been added for decreasing oxygen content between each of the spectra.

In order to confirm that the changes seen in the L_3 edge XANES as a function of oxygen content are of electronic origin, we also obtained Pr L_1-edge data, which correspond to a $2s$ to $6p$ transition, for a selected number of samples, as shown in Fig. 3. The peak, labeled B in Fig. 1, is not apparent in the L_1-edge data, confirming that the peak seen in the L_3-edge data is of electronic origin, and is not simple EXAFS.[29] The shift of the $2s$-$6p$ transition of approximately 4 eV (Ref. 30) between the weakly and strongly oxygenated samples lends further support to our statement that the Pr electronic configuration changes with doping, in accordance with the interpretation of the L_3-edge XANES.

B. Ca doping

X-ray diffraction results on $Pr_{1.05-x}Ca_xBa_{1.95}Cu_3O_7$ shown in Fig. 4 demonstrate a continuous reduction of the lattice constants for increasing Ca content. This smooth re-

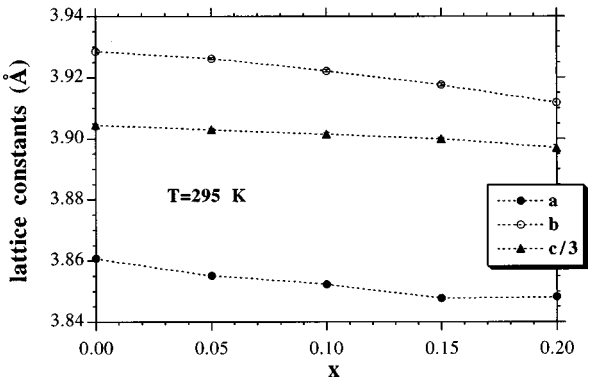

FIG. 4. Lattice constants at room temperature as a function of doping, for Ca doping in $Pr_{1.05-x}Ca_xBa_{1.95}Cu_3O_{7-\delta}$.

TABLE I. Selective interatomic distances found with neutron powder diffraction in $Pr_{1.05-x}Ca_xBa_{1.95}Cu_3O_7$ at 25 K for $x \neq 0$ and for $x=0$ taken from Ref. 31 (10 K).

	R-O(2) (Å)	*R*-O(3) (Å)	average buckling angle (°)	Cu(2)-Cu(2) (Å)	*a* (Å)	*b* (Å)	*c* (Å)
$x=0$	2.454 (8)	2.458 (8)	166.6 (4)	3.45 (1)	3.863 (1)	3.918 (1)	11.650 (1)
$x=0.05$	2.448 (5)	2.415 (5)	163.5 (3)	3.494 (7)	3.8413(1)	3.9168(1)	11.6547(2)
$x=0.15$	2.441 (7)	2.414 (7)	163.7 (3)	3.482 (9)	3.8358 (1)	3.9094(1)	11.6449(3)

duction indicates that Ca is incorporated into the lattice over the studied x range. Analysis of neutron diffraction data indicates an anomalously short Pr-O(2) distance [where O(2) represents the planar oxygen along b], which does not significantly change with Ca doping. Selected bond distances, obtained from a Rietfeld refinement of low temperature neutron diffraction data, are listed in Table I. This anomalously short distance has been previously observed for the $x=0$ compound.[5,31] In addition, the buckling angle of Cu(2)-O(2)-Cu(2), where Cu(2) is the planar Cu, does not significantly differ from that of the superconducting analogues. It does, however, remain smaller than that found[5,31] in $PrBa_2Cu_3O_7$. The Ca^{2+}, with an ionic radius of 1.12 Å in eightfold coordination,[32] replaces Pr^{3+}, with an ionic radii of 1.14 Å. The substitution of a slightly smaller ion for Pr should lead to a slight contraction of the lattice, in accordance with observation. However, the Pr-O(2) distance is distinctly shorter than that anticipated from simple ionic radii considerations. This result is consistent with either increased Pr-O orbital overlap or small changes in Pr valence with increasing Ca^{2+}. These results are similar to those found above for oxygen doping.

The Pr L_3-edge XANES data of the $Pr_{1.05-x}Ca_xBa_{1.95}Cu_3O_7$ samples are shown in Fig. 5. Peak B is seen to increase in intensity with increasing Ca concentration. The increase in the relative intensity of peak B with increased Ca doping is a smooth continuation of the trend established in the oxygenated samples. This change in peak B is interpreted as a further increase of the Pr valence or hybridization, an interpretation which is in agreement with the results from x-ray and neutron diffraction. The Pr L_1-edge data for the Ca-doped samples are shown in Fig. 6. Again, a slight increase in the transition energy with doping is observed. This shift of the $2s$-$6p$ (L_1 edge) transition again supports the interpretation that changes in the L_3 edge are of electronic origin.

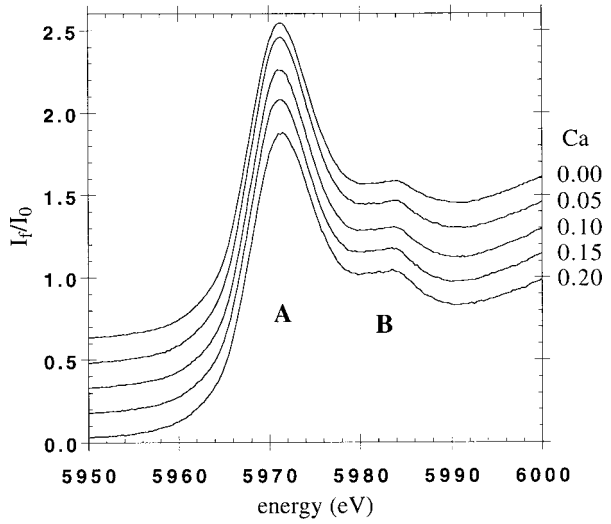

FIG. 5. Pr L_3-edge XANES of $Pr_{1.05-x}Ca_xBa_{1.95}Cu_3O_{7-\delta}$ for different Ca dopings x taken in fluorescence mode. An offset of 0.15 has been added for decreasing oxygen content between each of the spectra. The features A and B are as in Fig. 2.

C. Diffraction anomalous fine structure (DAFS)

Experiments on $PrBa_2Cu_3O_7$ can be vitiated by the presence of impurity phases, the most common of which, PrO_2 and $BaPrO_3$, contain tetravalent Pr. These impurities may not be detectable in standard x-ray diffraction patterns, either because they are not present in sufficient quantities, they have small particle sizes, or because they may not be well crystallized. In order to confirm the single-phase nature of our XANES sample and to demonstrate that the changes observed in the electronic properties of Pr originate from within the material of interest, we have employed diffraction anomalous fine structure (DAFS) spectroscopy.[33] In a DAFS experiment, the Bragg intensities of a particular reflection are measured as a function of energy, across an absorption edge of the element of interest. The Bragg intensities contain information analogous to a XANES spectrum, however the data are weighted by the structure factor for the specific reflection that is being monitored.

In this context, we have collected XRD diffraction patterns at energies around the Pr L_3 absorption edge. As an example, the normalized average intensities of the [213] and [123] reflections are shown in Fig. 7. The scattering factor of a resonant ion is given by $f_a = f_{0a} + f'_a + i f''_a$, with f''_a, f'_a,

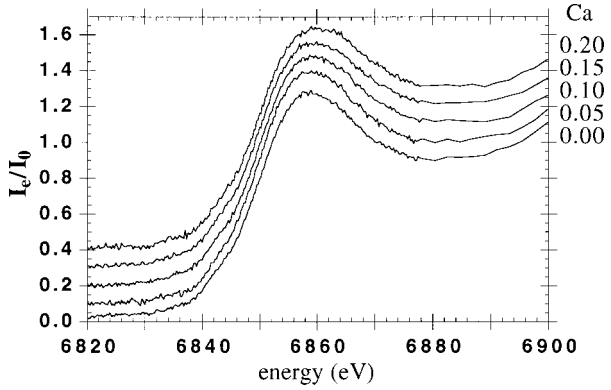

FIG. 6. Pr L_1-edge XANES of $Pr_{1.05-x}Ca_xBa_{1.95}Cu_3O_{7-\delta}$ for different Ca concentrations, taken in fluorescence mode. An offset of 0.1 has been added for decreasing oxygen content between each of the spectra.

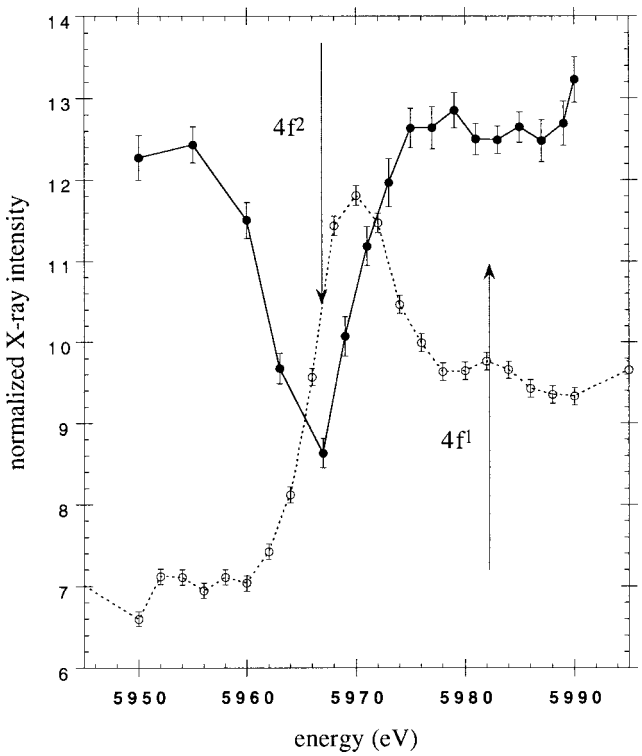

FIG. 7. Diffracted x-ray intensity (filled circles) and x-ray fluorescence intensity (open circles) of $Pr_{1.05}Ba_{1.95}Cu_3O_{6.97}$. The lines are guides to the eye. The arrows correspond to the main contributions of the $4f^1$ and $4f^2$ electronic configurations of Pr.

and f_{0a} the imaginary, real, and atomic parts of the scattering length, respectively. Because the Pr contribution to these reflections is purely real (f'_a), the diffracted intensity strongly decreases for the electronic $2p$-$5d$ transition at resonance. Also shown in Fig. 7 is the XANES absorption spectrum, which is extracted from the background intensity (fluorescence). The observed shift of the anomalous scattering DAFS-edge energy relative to the fluorescence XANES edge confirms that the DAFS scattering is dominated by the real component. The inflection point in the fluorescence data corresponds roughly to the minimum observed in the diffracted intensity, as expected in a simple atomiclike picture. Therefore, we interpret the source of the weak feature in the DAFS data at approximately 5985 eV as the $4f^1$ contribution of Pr (peak B). This result confirms that the higher-valency Pr contribution originates from the crystallographic $Pr_{1.05}Ba_{1.95}Cu_3O_7$ structure and is therefore intrinsic to $Pr_{1.05}Ba_{1.95}Cu_3O_{7-\delta}$. Unfortunately, the data do not have sufficient statistics to separate contributions from the two possible Pr sites, as would be required for a site-selective valence determination. More detailed investigations on this subject are currently underway.

DISCUSSION

It is clear from both oxygen-doped $Pr_{1.05}Ba_{1.95}Cu_3O_{7-\delta}$ and Ca-doped $Pr_{1.05-x}Ca_xBa_{1.95}Cu_3O_{7-\delta}$ that the Pr electronic structure, as probed by XANES spectroscopy, is influenced by changes in dopant concentrations. Confirmation that these changes occur in the material of interest, and not in an impurity phase, is obtained from the DAFS results. The

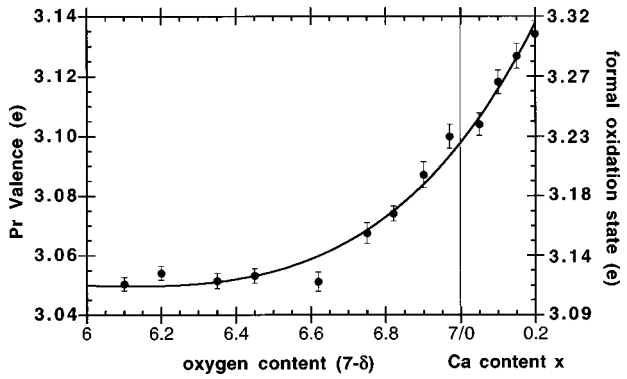

FIG. 8. Pr valence and formal oxidation state in $Pr_{1.05-x}Ca_xBa_{1.95}Cu_3O_{7-\delta}$, as a function of oxygen and Ca doping. The thick line serves as a guide to the eye, whereas the vertical line divides the x scale into oxygen (left side) and Ca doping (right site) regimes.

data from all samples are consistent with an essentially trivalent Pr that has a slightly modified electronic structure, the magnitude of which is dependent on dopant level.

There are two possible models that can be used to interpret these results. One model assumes that Pr has an intermediate valence that is changing with dopant concentration. The other model assumes a hybridization of Pr f states with ligand CuO planar states of the appropriate symmetry. It is not possible to distinguish between these models from the L_3 edge data.

An analysis of the XANES data shows that the electronic configuration of the Pr ions is unaffected by oxygen doping in the low concentration regime. This result is consistent with the picture that at low dopant levels the carriers introduced by doping go to the CuO chain states, whose states are physically removed from the Pr ions. For higher oxygen concentrations, the Pr valence increase is approximately linear with increasing oxygen content. This increase continues rather smoothly for Ca doping, despite the difference in formal charges introduced by these two ions. From simple chemical considerations, the Cu will be fully oxidized to Cu^{2+} at approximately δ=0.6. Therefore, at higher oxygen (or Ca) concentrations, the carriers are expected to go into the CuO planes. This change in carrier density then affects the hybridization, or charge transfer, to the Pr ions. It is to this change that the XANES spectra are sensitive. From the difference in formal charges introduced by oxygen and Ca, a much smaller increase in Pr valence for Ca compared to oxygen doping would be expected in the highly doped region. The similar valence increase in this region is consistent with the model that half of the holes introduced by oxygen doping remain on the apex oxygen, as suggested by a recent XAS study[34] on single crystals of $Y_{1-x}Ca_xBa_2Cu_3O_{7-\delta}$. The number of holes localized by Pr, as found by our study, is similar to the hole count in the CuO_2 planes, determined by neutron spectroscopy,[35] whereas the oxygen XAS results obtained a slightly larger number,[34] and bond valence sum arguments yield a slightly smaller value.[36]

Although the results are presented in Fig. 8 as changes in the Pr valence with doping, the changes in the Pr XANES are consistent with theories that involve either charge transfer or Pr-CuO hybridization. In either case, the changes in the Pr electronic properties observed in the XANES data

clearly demonstrate a strong interaction between the *f*-ion states and the CuO states that hold the superconducting carriers. It is this interaction that results in both the high Neél temperature and the suppressed superconductivity in these Pr-containing samples.

These results can be compared with inelastic neutron scattering experiments on $PrBa_2Cu_3O_7$, which show an unusually broad intensity distribution in the magnetic scattering.[6,7] These broadened peaks are an unambiguous signature of an interaction between the magnetic $4f$ states and ligand orbitals. The anomalously high T_N is an additional indication of such an interaction.

It is interesting to compare the strength of the superexchange interaction obtained from an analysis of the crystal field states with results obtained from the XANES. We use a simple mean-field approach to obtain a quantitative estimate of the magnetic-exchange interaction λ, which is obtained from $\lambda = 1/\chi(T_N)$, where χ is the paramagnetic susceptibility. The susceptibility, in turn, can be calculated from the crystalline-electric field potential of the Pr ions.[37] The corresponding values for λ are 0.25 and 0.125 meV for $\delta = 0.9$ and 0.03, respectively. The factor of two difference in λ with different oxygen contents indicates that the difference in Pr-O overlap *t*, which is proportional to t^4, between the doped and the undoped compounds is much smaller, indicating a complex relation between the overlap and the valence.

It is informative to compare the results found here with those of Pr in the $Pb_2Sr_2R_{1-x}Ca_xCu_3O_8$ series. The material $Pb_2Sr_2R_{1-x}Ca_xCu_3O_8$ (R=Y, rare earth) is doped solely by the replacement of trivalent R by divalent Ca, and optimal doping is achieved at approximately 50% substitution, with a superconducting transition temperature of approximately 70 K for polycrystalline samples.[38] In contrast to the $RBa_2Cu_3O_{7-\delta}$ series, the Pr analog of the $Pb_2Sr_2R_{1-x}Ca_xCu_3O_8$ series only weakly suppresses T_c (T_c is approximately[39] 60 K). From an analysis of the Pr L_3 edge absorption data[39] from $Pb_2Sr_2Pr_{0.5}Ca_{0.5}Cu_3O_8$, we obtain a valence of Pr of 3.029 ± 0.003, which is lower than that determined for optimally doped $PrBa_2Cu_3O_{6.9}$. By assuming that the feature B in the undoped $x=0$ compound reflects the strength of the hybridization between Pr and the CuO_2 bands, the obtained values of 3.045 and 3.029 for $x=0$ and $x=0.5$, respectively, can be interpreted in terms of a decreasing hybridization for increasing Ca content, in contrast to an increasing hybridization for increasing doping (oxygen, Ca) in the $PrBa_2Cu_3O_{7-\delta}$ structure. It has been shown that the average splitting of the magnetic ''quasitriplet'' ground state of the $4f$ electrons is enlarged for Ca-doped $Pb_2Sr_2Pr_{0.5}Ca_{0.5}Cu_3O_8$ compared to the undoped material or to $PrBa_2Cu_3O_{7-\delta}$, resulting in a reduced magnetic ground state.[40] This result has been used to argue that the increased splitting of the quasitriplet ground state may compete with hybridization, thereby reducing the ability of the Pr ions to form a higher valence. Models such as the one proposed by Fehrenbacher and Rice[10] are based on the valence state of Pr by assuming a hybridization of the triplet ground state $4f_{z(x^2-y^2)}$ and the oxygen $2p_\pi$ orbitals (a linear combination of $Pr^{3+} + Pr^{4+}\underline{L}$ wave functions) makes such a scenario likely. The increased Pr-O distance for $Pb_2Sr_2Pr_{0.5}Ca_{0.5}Cu_3O_8$ (Ref. 39) compared to the undoped $Pb_2Sr_2PrCu_3O_8$, indicates again that the electronic properties of Pr are better approximated by a single-ion trivalent model for the Ca doping of the Pb-based samples than for the $Pr_{2-x}Ca_xBa_2Cu_3O_7$ samples, where the distance is constant. Samples with higher Ca doping, obtained only as thin films, again show increased lattice spacings (suggesting an increased Pr-O distance), and therefore an effectively smaller hybridization. This argument may explain the higher superconducting transition temperature found for $Pr_{0.5}Ca_{0.5}Ba_2Cu_3O_7$ ($T_c = 47$ K) compared to $Y_{0.5}Pr_{0.5}Ba_2Cu_3O_7$ ($T_c = 22$ K).

CONCLUSIONS

Pr L_3-edge XANES data are seen to change as a function of both oxygen and Ca doping in $Pr_{1-x}Ca_xBa_2Cu_3O_{7-\delta}$. DAFS data confirm that the observed changes do not arise from the presence of an impurity phase. The changes seen in the Pr XANES are evidence that the electronic ground state of Pr is changing with dopant concentration. We have used a model based on literature precedent to analyze the data. This model quantifies changes in the XANES spectra in terms of a changing Pr valence, although changes in the hybridization of the Pr $4f$ states with the planar CuO bands cannot be ruled out. From this modeling, the valence of Pr is seen to increase with increasing oxygen content, but only for samples with $\delta \leqslant 0.6$. Trends seen with increasing oxygen content continue smoothly with the Ca doping of fully oxygenated samples. The quantitative values of the Pr valence build a base for further modeling which describes the exceptional electronic and magnetic properties of Pr in layered cuprates.

ACKNOWLEDGMENTS

We would like to acknowledge the help of F. Fauth in the neutron diffraction experiments. This work has been supported in part (L.S. and S.R.W.) by the U.S. DOE, BES-Chemical Sciences, under Contract No. W-31-109-ENG-38. Research conducted at the National Synchrotron Light Source is supported by the U.S. DOE, Divisions of Chemical and Materials Sciences.

[1] L. Soderholm, K. Zhang, D. G. Hinks, M. A. Beno, J. D. Jorgenson, C. U. Segre, and I. K. Schuller, Nature (London) **328**, 604 (1987).

[2] W.-H. Li, J. W. Lynn, S. Skanthakumar, and T. W. Clinton, Phys. Rev. B **40**, 5300 (1989).

[3] J. W. Lynn and S. Skanthakumar, in *Handbook on the Physics and Chemistry of Rare Earths*, edited by K. A. Gschneidner, Jr. and L. Eyring (North-Holland, Amsterdam, in press).

[4] P. Fischer and M. Medarde, in *Neutron Scattering in Layered Copper-Oxide Superconductors*, edited by A. Furrer (Kluwer Academic Publishers, Dordrecht, 1998), p. 261.

[5] M. Guillaume, P. Allenspach, J. Mesot, B. Roessli, U. Staub, P.

Fischer, and A. Furrer, Z. Phys. B **90**, 13 (1993).
[6] L. Soderholm, C.-K. Loong, G. L. Goodman, and B. D. Dabrowski, Phys. Rev. B **43**, 7923 (1991).
[7] H.-D. Jostarndt, U. Walter, J. Harnischmacher, J. Kalenborn, A. Severing, and E. Holland-Moritz, Phys. Rev. B **46**, 14 872 (1992).
[8] A. T. Boothroyd, S. M. Doyle, and R. Osborn, Physica C **217**, 425 (1993).
[9] Y. Dalichaouch, M. S. Torikachvili, E. A. Early, B. W. Lee, C. L. Seaman, K. N. Yang, H. Zhou, and M. B. Maple, Solid State Commun. **65**, 1001 (1988).
[10] R. Fehrenbacher and T. M. Rice, Phys. Rev. Lett. **70**, 3471 (1993).
[11] A. I. Liechtenstein and I. I. Mazin, Phys. Rev. Lett. **74**, 1000 (1995).
[12] G. Y. Guo and W. M. Temmerman, Phys. Rev. B **41**, 6372 (1990).
[13] H. B. Radousky, J. Mater. Res. **7**, 1917 (1992).
[14] H. A. Blackstead and J. D. Dow, Phys. Rev. B **51**, 11 830 (1996).
[15] Z. Zou, J. Ye, K. Oka, and Y. Nishihara, Phys. Rev. Lett. **80**, 1074 (1998).
[16] C. R. Fincher, Jr. and G. B. Blanchet, Phys. Rev. Lett. **67**, 2902 (1991).
[17] J. Röhler, in *Handbook on the Physics and Chemistry of Rare Earths*, edited by K. A. Gschneider, Jr., L. Eyring, and S. Hüfner (North-Holland, Amsterdam, 1987), Vol. 10, p. 453.
[18] U. Neukirch, C. T. Simmons, P. Sladeczek, C. Laubschat, O. Strebel, G. Kaindl, and D. Sarma, Europhys. Lett. **5**, 567 (1988).
[19] E. E. Alp, G. K. Shenoy, L. Soderholm, G. L. Goodman, D. G. Hinks, and B. W. Veal, in *High-Temperature Superconductors*, edited by M. B. Brodsky, R. C. Dynes, K. Kitawa, and H. L. Tuller, MRS Symposia Proceedings No. 99 (Materials Research Society, Pittsburgh, 1988), pp. 177–182.
[20] C. H. Booth, F. Bridges, J. B. Boyce, T. Claeson, Z. X. Zhao, and P. Cervantes, Phys. Rev. B **49**, 3432 (1994).
[21] S. Horn, J. Cai, S. A. Shaheen, Y. Jeon, M. Croft, C. L. Chang, and M. L. d. Boer, Phys. Rev. B **36**, 3895 (1987).
[22] M. Khaled, N. L. Saini, K. B. Garg, and F. Studer, Solid State Commun. **100**, 773 (1996).
[23] G. Hilscher, T. Holubar, G. Schaudy, J. Dumschat, M. Strecker, G. Wortmann, X. Z. Wang, B. Hellebrand, and D. Bäuerle, Physica C **224**, 330 (1994).
[24] F. W. Lytle, G. v. d. Laan, and R. B. Greegor, Phys. Rev. B **41**, 8955 (1990).
[25] M. Merz, N. Nuecker, E. Pellegrin, P. Schweiss, and S. Schuppler, Phys. Rev. B **55**, 9160 (1997).
[26] M. Gasgnier, G. Schiffmacher, L. Albert, P. E. Caro, H. Dexpert, J. M. Esteva, C. Blancard, and R. C. Karnatak, J. Less-Common Met. **156**, 59 (1989).
[27] A. Bianconi, A. Marcelli, H. Dexpert, R. Karnatak, A. Kotani, T. Jo, and J. Petiau, Phys. Rev. B **35**, 806 (1987).
[28] Z. Hu, S. Bertram, and G. Kaindl, Phys. Rev. B **49**, 39 (1994).
[29] F. W. Lytle and R. B. Greegor, Appl. Phys. Lett. **56**, 192 (1900).
[30] G. Kaindl, G. Schmiester, E. V. Sampathkumaran, and P. Wachter, Phys. Rev. B **38**, 10 174 (1988).
[31] M. Guillaume, P. Allenspach, W. Henggeler, J. Mesot, B. Roessli, U. Staub, P. Fischer, A. Furrer, and V. Trounov, J. Phys.: Condens. Matter **6**, 7963 (1994).
[32] A. D. Shannon, Acta Crystallogr., Sect. A: Cryst. Phys., Diffr., Theor. Gen. Crystallogr. **32**, 751 (1976).
[33] H. Stragier, J. O. Cross, J. J. Rehr, L. B. Sorensen, C. E. Bouldin, and J. C. Woicik, Phys. Rev. Lett. **69**, 3064 (1992).
[34] M. Merz, N. Nücker, P. Schweiss, S. Schuppler, C. T. Chen, V. Chakarian, J. Freeland, Y. U. Idzerda, M. Kläser, G. Müller-Vogt, and T. Wolf, Phys. Rev. Lett. **80**, 5192 (1998).
[35] J. Mesot, P. Allenspach, U. Staub, A. Furrer, H. Mutka, R. Osborn, and A. Taylor, Phys. Rev. B **47**, 6027 (1993).
[36] R. J. Cava, A. W. Hewat, E. A. Hewat, B. Battlogg, M. Marezio, K. M. Rabe, J. J. Krajewski, W. F. Peck, Jr., and L. W. Rupp, Jr., Physica C **165**, 419 (1990).
[37] U. Staub and L. Soderholm, in *Handbook on the Physics and Chemistry of Rare Earths* (Ref. 3).
[38] L. F. Schneemeyer, R. J. Cava, A. C. W. P. James, P. Marsh, T. Siegrist, J. V. Waszczak, J. J. Krajewski, W. P. Peck, R. L. Opila, S. H. Glarum, M. J. H. R. Hull, and J. M. Bonar, Chem. Mater. **1**, 548 (1989).
[39] S. Skanthakumar and L. Soderholm, Phys. Rev. B **53**, 920 (1996).
[40] U. Staub, L. Soderholm, S. Skanthakumar, R. Osborn, and F. Fauth, Europhys. Lett. **39**, 663 (1997).